Dispersion of Potassium Nitrate and the Resulting Strong Basicity on Zirconia

Ying Wang, Wen Yu Huang, Yuan Chun, Jia Rong Xia, and Jian Hua Zhu*

Department of Chemistry, Nanjing University, Nanjing 210093, China

Received March 9, 2000. Revised Manuscript Received October 24, 2000

A novel solid superbase is derived from zirconia-supported potassium nitrate. Dispersion and decomposition of potassium nitrate on zirconia were investigated and compared with that on alumina to explore the effect of the support on the preparation of solid strong bases. Spontaneous dispersion capacity of KNO_3 on ZrO_2 was found to be 8.1 K^+ nm^{-2}, very close to that of a vacant site on ZrO_2. An unusually strong basicity was generated on ZrO_2 through decomposition of the loaded KNO_3 that began around 613 K, enhancing the catalytic activity of ZrO_2 in *cis*-but-2-ene isomerization at 273 K. Moreover, KNO_3/ZrO_2 samples, except 34% KNO_3/ZrO_2, possessed a base strength of $H_- = 27.0$ that was characteristic of solid superbases.

Introduction

Preparation of solid superbases is a developing area attracting more and more attention because superbases possess high activity in various reactions under mild conditions and minimize the production of pollutants. However, most of the known superbases are inconvenient for industrial application because they are difficult to prepare[1] and are oxygen-sensitive.[2] Therefore, preparation of novel superbases becomes the key step for developing environmentally benign base catalytic processes. Recently, we reported a new method to prepare superbases by loading KNO_3 on zeolite KL[3] or γ-Al_2O_3.[4] No basicity formed on these composites in ambient conditions because the guest−host interaction could not make KNO_3 decompose so that CO_2 contamination from the atmosphere could be avoided in storage of KNO_3/Al_2O_3 or KNO_3/KL inactivated. Those strong basic sites needed to be active centers only formed in the activation prior to reaction; therefore, they keep high efficiency in catalytic process.[4] Further investigation revealed a relationship between loaded KNO_3 and generated basicity over the composite: If the amount of KNO_3 loaded was below the spontaneous dispersion threshold, it could be well dispersed and provoke a basic strength (H_-) of 18.4 on alumina. When the amount of KNO_3 was above the threshold, it only dispersed and decomposed during the evacuation at 873 K but generated some unusually strong basic sites with a strength (H_-) of 27.0. For another type of support, such as zeolite NaY and $AlPO_4$-5, KNO_3 was highly dispersed but difficult to decompose because of the lack of an octahedral vacant site in zeolite provided for insertion of the K^+ ion.[4]

However, there are still many uncertainties existing around KNO_3-supported materials. It is unclear at what temperature the loaded KNO_3 begins to decompose. Moreover, is it possible to apply this method for creating superbasic sites on other oxides such as zirconia, which also have an octahedral vacant site in its structure? Is the resulting basicity on KNO_3/ZrO_2 the same as that on KNO_3/Al_2O_3? If not, what causes the difference? Zirconia is an important catalyst and carrier in industry, having both acidity−basicity and redox properties, and it plays an unusual role in the direct synthesis of dimethyl carbonate from CO_2 and methanol owing to its especial properties.[5] It is well-known that zirconia has surface acidity equivalent to about 100% H_2SO_4 after being modified with SO_4^{2-} [6−8] and it could be converted to a solid strong base by use of KF modification,[9] but there is no open literature concerning the superbases based on ZrO_2. This prompts us to load KNO_3 onto ZrO_2 and to explore the dispersion and decomposition of KNO_3 by use of XRD, XPS, and temperature-programmed decomposition (TPDE) methods.

Experimental Section

Samples of KNO_3/ZrO_2 were prepared in a "dry" impregnation process similar to that for KNO_3/Al_2O_3 .[4] ZrO_2 (Toray Ltd., SA = 120 m^2 g^{-1}) and KNO_3 were ground at a given weight ratio in mortar to mix them, followed by the addition of 0.5 mL g^{-1} distilled water. The paste was kneaded for 10 min, dried at 383 K for 12 h, and finally crushed to particles in 20−40 mesh. X-ray diffraction patterns of these samples were obtained with a Rigaku D/max-rA diffractometer employing Cu Kα radiation, and the X-ray tube was operated at 50 kV

(1) Baba, T.; Handa, I.; Ono, Y. *J. Chem. Soc., Faraday Trans.***1994**, *90*, 187.
(2) Tanabe, K.; Yoshii, N.; Hattori, H. *J. Chem. Soc., Chem. Commun.***1971**, 464.
(3) Zhu, J. H.; Chun, Y.; Wang, Y.; Xu, Q. H. *Mater. Lett.* **1997**, *33*, 207.
(4) Zhu, J. H.; Wang, Y.; Chun, Y.; Wang, X. S. *J. Chem. Soc., Faraday Trans.***1998**, *94*, 1163.
(5) Tomishige, K.; Sakaihori, T.; Ikeda, Y.; Fujimoto, K. *Catal. Lett.* **1999**, *58*, 225.
(6) Umansky, B.; Engelhardt, J.; Hall, W. K. *J. Catal.* **1991**, *127*, 128.
(7) Adeeva, V.; de Haan, J. W.; Janchen, J.; Lei, G. D.; Schunemann, G.; van de Ven, L. J. M.; Sachtler, W. M. H.; Santen, R. A. *J. Catal.* **1995**, *151*, 364.
(8) Yamaguchi, T.; Tanabe, K. *Mater. Chem. Phys.* **1986**, *16*, 67.
(9) Zhu, J. H.; Hattori, H.; Kita, H. *Chin. Chem. Lett.* **1995**, *6*, 1005.

10.1021/cm000213n CCC: $20.00
Published on Web 01/27/2001

and 150 mA for measuring samples. X-ray photoelectron spectra (XPS) were recorded with a V.G. Escalab MK II system equipped with a hemispherical electron analyzer, and C(1s) (285.0 eV) was taken as a reference to calculate the binding energy (E_b).

TPDE of supported KNO_3 was carried out in a flow reactor.[10] A sample of 5 mg was heated in a flow of N_2 (30 mL min^{-1}) from 298 to 873 K at a rate of 8 K min^{-1}. The NO_x ($x < 2$) liberated in the process was converted to NO_2 by passing NO_x through a CrO_3 tube and the product was detected by the colorimetric method (CM),[11] representing the amount of KNO_3 decomposed. For determination of the NO_2 in the liberated gas product, the CrO_3 tube was removed so that the NO_x ($x < 2$) was invisible. A TPDE-MS experiment was carried out in the procedure described previously.[12] In a CO_2-TPD experiment, a 50-mg sample was heated in a flow of He (99.999%) at a rate of 8 K min^{-1} to 873 K and kept at 873 K for 2 h to decompose KNO_3. Prior to adsorption of CO_2 (99.999%) at 298 K, blank TPD was carried out from 298 to 873 K to confirm no desorption occurred. After the physical adsorbed CO_2 was purged by a He flow at 298 K for 1−2 h, CO_2-TPD was performed at the rate of 8 K min^{-1} up to 873 K, and the CO_2 liberated was detected by an "on-line" Varian 3700 chromatograph.[4] When the CO_2-TPD experiment was finished, the sample was shaken in 0.02 M aqueous HCl (5 mL), and the remaining acid was then titrated with standard base (0.02 M aqueous NaOH) to measure the total basicity of the sample. The basic strength of the KNO_3/ZrO_2 sample was measured by use of a Hammett indicator in a manner similar to that described previously.[3]

Dehydrogenation of propa-2-nol at 673 K and isomerization of *cis*-but-2-ene at 273 K were employed to evaluate catalytic properties of KNO_3/ZrO_2. The former reaction was carried out in a conventional flow reactor with a WHSV of 1.88 h^{-1}.[4] A 50-mg portion of the catalyst was activated at 873 K for 2 h in a flow of N_2 prior to reaction. Nitrogen was used as the carrier gas, and the total pressure was 0.1 MPa while the partial pressure of propa-2-nol was 9.1 kPa. Reaction products were analyzed by an on-line Varian 3700 gas chromatograph equipped with a Porapak T column ($\Phi 3 \times 4000$ mm) and a TCD, and analysis data were normalized by using a HP3390A integrator. A glass closed recirculation reactor, connected to a conventional vacuum line and to a GC, was employed for the isomerization of butene at 273 K.[12] The catalyst was evacuated under $\approx 10^{-3}$ Pa at an elevated temperature for 2 h prior to reaction. The reaction mixture was occasionally separated by a 5-m column packed with VZ-7 that operated at room temperature and was analyzed by an on-line gas chromatograph equipped with TCD, and the initial ratio of *trans*-but-2-ene to but-1-ene (t-B/1-B) in the products was obtained by extrapolation to zero conversion.

Results and Discussion

A. Dispersion and Decomposition of KNO_3 on Zirconia. The zirconia used as the support was a porous material with a pore volume of 0.23 mL g^{-1} and an average pore size of 6.66 nm. Two crystal phases, monoclinic baddeleyite and tetragonal form, existed in the ZrO_2, and the former had an intensity stronger than the latter. Figure 1 shows XRD patterns of ZrO_2 heated at various temperatures in air. A monoclinic phase developed as the temperature increased while the tetragonal phase disappeared after calcination at 973 K, giving proof that tetragonal crystal in ZrO_2 is a metastable phase. Figure 1 also shows the effect of heat treatment on a 20% KNO_3/ZrO_2 sample. Calcination at

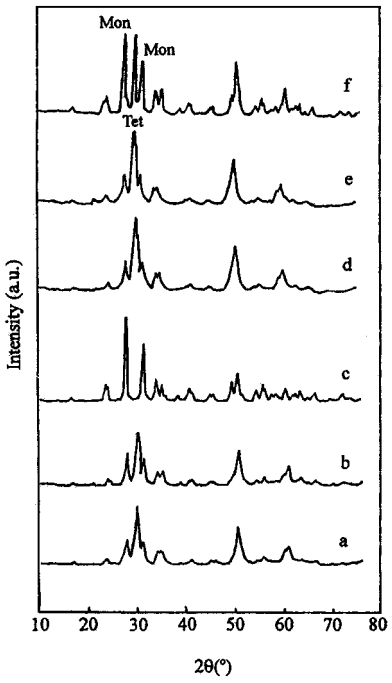

Figure 1. XRD patterns of ZrO_2 (a) dried at 383 K, calcined at (b) 773 K and (c) 973 K, and 20% KNO_3/ZrO_2 (d) dried at 383 K, calcined at (e) 773 K and (f) 973 K.

773 K caused no change in the relative intensity of the monoclinic phase, but calcination at 973 K made the phase develop quickly. However, the metastable tetragonal crystalline phase was maintained to a great degree, even when the sample was heated at 973 K, similar to the stabilization of tetragonal crystal after the incorporation of Ca^{2+} in ZrO_2.[13] Those Ca^{2+} ions were assumed to occupy the position of Zr^{4+} and formed an O^{2-} vacancy; therefore, these K^+ ions were inferred to occupy the position of octa-coordinated Zr^{4+}, which is more stable than the hepta-coordinated Zr^{4+} because of the interaction of K salt with zirconia.

Figure 2 shows the XRD patterns of KNO_3/ZrO_2. The samples 7.5% KNO_3/ZrO_2 and 14% KNO_3/ZrO_2 had XRD patterns almost identical to that of ZrO_2, characterized by the peaks at 2θ of 30.2°, 50.2°, and 60.2°, representing the tetragonal form of zirconia.[14] When the amount of KNO_3 rose over 20 wt %, its characteristics emerged in the patterns near 2θ of 23.6°, 29.4°, and 33.8°, respectively, though parts of them were overlapped by the XRD peaks of ZrO_2, representing the residual phase of KNO_3. On the basis of these results, it is clear that the spontaneous dispersion capacity of KNO_3 on ZrO_2 is about 14 wt % because the loaded KNO_3 can be well dispersed and no distortion occurred in the structure of ZrO_2. The corresponding surface concentration of K^+ for the dispersion capacity was 8.1 nm^{-2}, close to the surface concentration of the vacant site on ZrO_2 (8.6 nm^{-2}).[15] Vacant sites play an important role in the interaction between guest ions and support because the K^+ ion of KNO_3 can penetrate the site of alumina during the preparation of KNO_3/Al_2O_3,[4,12] accelerating dissociated dispersion and decomposition of KNO_3 to form

(10) Shen, B.; Chun, Y.; Zhu, J. H.; Wang, Y.; Wu, Z.; Xia, J. R.; Xu, Q. H. *Physchemcomm.* **1999**, 3.
(11) Saltzman, B. E. *Anal. Chem.* **1954**, *26*, 1949.
(12) Yamaguchi, T.; Zhu, J. H.; Wang, Y.; Komatsu, M.; Ookawa, M. *Chem. Lett.***1997**, 989.
(13) Duwez, P.; Brown, F. H. *J. Am. Ceram. Soc.* **1952**, *35*, 109.
(14) JCPDS file number 17-0932.
(15) Liu, Z.; Dong, L.; Ji, W.; Chen, Y. *J. Chem. Soc., Faraday Trans.* **1998**, *94*, 1137.

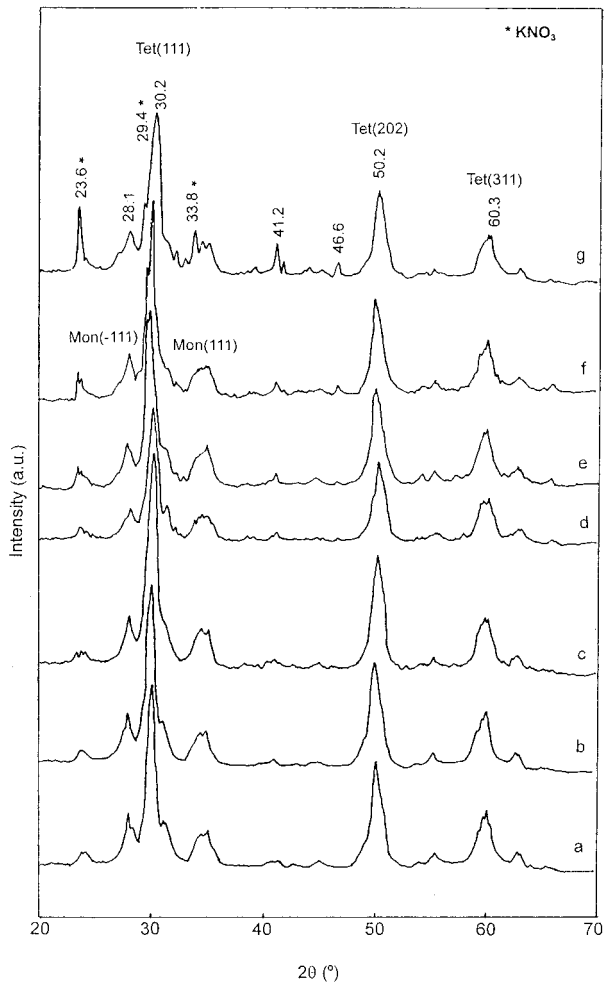

Figure 2. XRD patterns of ZrO_2 (a) before and after being loaded with KNO_3 of (b) 7.5 wt %, (c) 14 wt %, (d) 20 wt %, (e) 25 wt %, (f) 30 wt %, (g) 34 wt % and dried at 383 K.

strong basic species in the activation process. A close relationship is thus observed between the amount of KNO_3 spontaneously dispersed and the vacant sites on Al_2O_3 .[4] Because such a relationship also existed with KNO_3/ZrO_2, dissociated dispersion of KNO_3 seemed to occur on zirconia. Different from KNO_3/Al_2O_3 samples where $K_2[Al(NO_3)_5]$ formed because of intensive interactions between KNO_3 and alumina,[4] no crystallized compound such as K_2ZrO_3 formed, even the loading amount of KNO_3 reached 34 wt % or the sample of 20% KNO_3/ZrO_2 was calcined at 773 K. One of the reasons for the difference was the intrinsic feature of ZrO_2 having smaller vacancies in its structure compared with those of γ-Al_2O_3 .[16]

Table 1 demonstrates the decomposition of KNO_3 loaded on ZrO_2 revealed by the TPDE-CM method. KNO_3 began to thermally decompose at 753 K,[10,17] and it started to decompose in the range of 613−683 K after being supported on zirconia, higher than that on Al_2O_3 (433−554 K) and zeolite NaY (510 K), KL (513 K), and mesoporous materials MCM-41 (507 K).[10] Among the products of KNO_3 decomposition, NO_2 was the only one detected below 673 K. In the case of KNO_3 loaded below

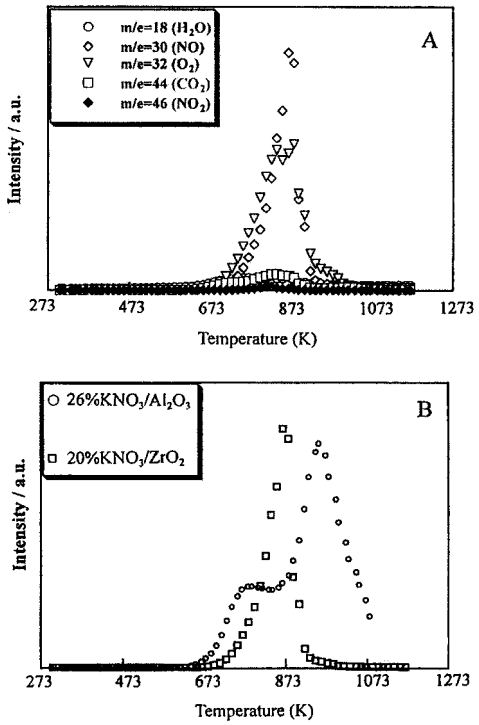

Figure 3. TPDE profile of (A) 27% KNO_3/ZrO_2 and (B) NO desorbed from 20% KNO_2/ZrO_2 and 26% KNO_3/Al_2O_3 samples.

the spontaneous dispersion threshold (14 wt %), NO_2 was the dominant product during the TPDE process. If the amount exceeded the threshold, the proportion of NO_x ($x < 2$) was close to that of NO_2, especially over 773 K, except for the 34% KNO_3/ZrO_2 sample. The 34% KNO_3/ZrO_2 sample showed the highest temperature to start KNO_3 decomposition (683 K) and the smallest decomposition percentage (1.8%) among the KNO_3/ZrO_2 samples. Consulting the XRD results mentioned above, it is obvious that well-dispersed KNO_3 can be easily decomposed owing to the interaction with ZrO_2, while for those KNO_3 that formed several layers on a support, a higher temperature is therefore needed. On the other hand, interaction of KNO_3 with ZrO_2 was proven to be weaker than that with Al_2O_3. KNO_3 began to decompose at 403 K on the 4% KNO_3/Al_2O_3 sample and about half (46%) decomposed in the TPDE process.[17] However, KNO_3 started to decompose at 548 K on the sample of 2.8% KNO_3/ZrO_2 with the same K^+ ion concentration (1.4 K^+ nm^{-2}), and the decomposition percentage was about one-fifth (21%).

To gain a deeper insight into the decomposition of KNO_3 on zirconia, the TPDE-MS technique was employed and Figure 3 shows the profiles of the KNO_3/ZrO_2 and KNO_3/Al_2O_3 samples. NO appeared on the spectrum of 27% KNO_3/ZrO_2 near 673 K, and it became predominant in the 723−973 K range with a maximum near 863 K. These NO species could be tentatively divided into two parts. One seemed derived from NO_2 during the mass detection process because the profile of O_2 had a development tendency similar to that of NO. Another might be that originally formed in KNO_3 decomposition because the mass signal of NO was much stronger than that of O_2 in the range of 823−873 K. NO_2 and CO_2 were also observed in the spectrum of 27% KNO_3/ZrO_2, but both were minor components. The former had an unclear weak peak at 813 K while the

(16) Gates, B. C.; Katzer, J. R.; Schuit, G. C. A. *Chemistry of Catalytic Processes*; McGraw-Hill: New York, 1979.
(17) Shen, B.; Chun, Y.; Zhu, J. H.; Xia, J. R.; Wang, Y.; Xu, Q. H. *Chin. J. Inorg. Chem.* **1999**, *15*, 351.

Table 1. Decomposition of KNO_3 Loaded on Zirconia

sample		7.5% KNO_3/ZrO_2	14% KNO_3/ZrO_2	20% KNO_3/ZrO_2	27% KNO_3/ZrO_2	34% KNO_3/ZrO_2
amount of KNO_3 loaded (mmol g^{-1})		0.743	1.386	1.980	2.673	3.366
Amount of NO_2 or NO_x ($x < 2$) Detected at Different Temperatures (mmol g^{-1})						
473−573 K	NO_x ($x < 2$)	0	0	0	0	0
NO_2	0	0	0	0	0	
573−673 K	NO_x ($x < 2$)	0	0	0	0	0
NO_2	0.004	0.003	0.004	0.001	0.004	
673−773 K	NO_x ($x < 2$)	0.002	0.001	0.024	0.006	0
NO_2	0.007	0.005	0.036	0.002	0.004	
773−873 K	NOx ($x<2$)	0.006	0.039	0.077	0.053	0.017
NO_2	0.121	0.110	0.010	0.045	0.037	
temperature at which KNO_3 starts to decompose (K)		613	623	613	613	683
amount of KNO_3 to be decomposed[a] (mmol g^{-1})		0.140	0.158	0.151	0.107	0.062
percentage of KNO_3 to be decomposed (%)		18.8	11.4	7.6	4.0	1.8

[a] Based on the amount of NO_x ($x < 2$) and NO_2 detected.

Table 2. XPS Analysis Data of Zirconia-Supported Potassium Nitrate

amount of KNO_3 loaded(wt %)	7.5	14.0	20.0	27.0	34.0
surface composition (by XPS)					
K (at. %)	3.39	3.91	3.93	5.96	8.21
O (at. %)	68.11	69.22	70.73	69.12	65.92
Zr (at. %)	28.49	26.87	25.35	24.92	20.93
N (at. %)	0	0	0	0	4.94
N/K ratio	0	0	0	0	0.60
K/Zr ratio	0.11	0.21	0.16	0.20	0.39
K/Zr ratio calculated	0.10	0.20	0.31	0.45	0.63

latter appeared around 673 K with a small peak near 823 K. Part of the loaded KNO_3 seemed to decompose on the sample in the drying process, generating some basic sites and adsorbing CO_2 from the atmosphere. Two differences were found in this experiment. Only one peak near 873 K was observed in the NO profile of 20% KNO_3/ZrO_2 or 27% KNO_3/ZrO_2, while the NO profile of 26% KNO_3/Al_2O_3 contained two evolution peaks at about 773 and 823 K (Figure 3B), resulting from the decomposition of $K_2Al(NO_3)_5$ and KNO_3 crystalline.[12] In addition, the decomposition of KNO_3 finished at about 973 K on KNO_3/ZrO_2 whereas it continued up to 1073 K on KNO_3/Al_2O_3. The lack of crystallized compound like K_2ZrO_3 on KNO_3/ZrO_2 could explain the absence of NO evolution below 773 K, but the reason decomposition of KNO_3 finished near 973 K instead of 1073 K was unclear. Reduced defects were reported to exist on zirconia[18] and redox could accelerate decomposition of KNO_3 ,[10] but a picture of the mechanism cannot be drawn and further investigation is desirable.

Table 2 lists XPS data of KNO_3/ZrO_2. For those supported KNO_3 samples <14 wt %, the surface K/Zr ratio measured by XPS was close to the theoretical value. When the amount of KNO_3 exceeded 14 wt %, the surface K/Zr ratio was only about half the theoretical value. Similar phenomena were found on KNO_3/Al_2O_3 samples and attributed to heterogeneous distribution of KNO_3 because most of the loaded KNO_3 located in the pore of the support.[4] Besides, no N(1s) signal was observed on KNO_3/ZrO_2 samples except for 34% KNO_3/ZrO_2 in the range of 410−390 eV where N(1s) of $NaNO_3$ or NH_4NO_3 was reported[19] and no Auger signal of

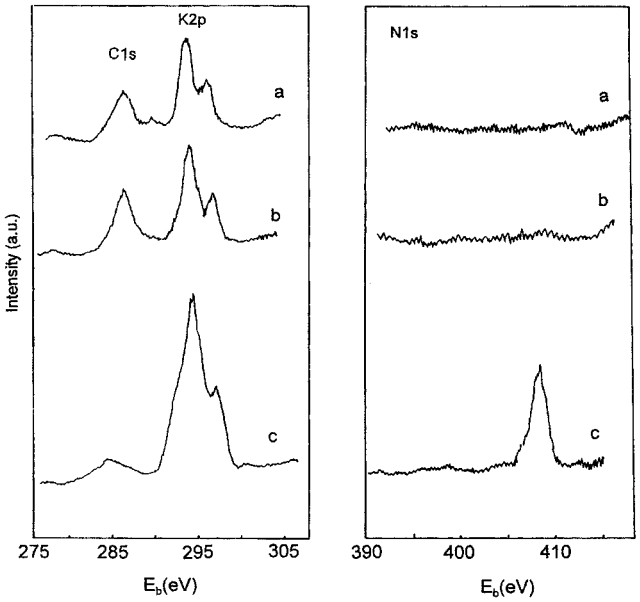

Figure 4. K(2p) and N(1s) signals on the XPS spectra of the powder sample of (a) 14% KNO_3/ZrO_2 and (b) 27% KNO_3/ZrO_2 and the pellet sample of (c) 27% KNO_3/ZrO_2.

nitrogen at all. The N(1s) peak appeared on the XPS spectrum of 34% KNO_3/ZrO_2 and the surface N/K ratio became 0.60 as seen in Table 2, close to that of KNO_3 (0.68). The absence of the N(1s) signal on XPS spectra has been reported on KNO_3/Al_2O_3 ,[4] KNO_3/SiO_2, KNO_3/NaY, KNO_3/KL, and $KNO_3/AlPO_4$[5−].[10] These phenomena cannot be simply attributed to the detection limitation because no such phenomenon was found in K(2p) signals on the XPS spectra (Figure 4). Assuming the dispersed species kept the form of KNO_3, there should be a similar concentration of N species on the sample as K species and they should be detected by an XPS test like that reported on the $LiNbO_3$-adsorbed NO.[20] The state of KNO_3 supported on ZrO_2 seems to be changed, probably because of the influence of X-ray radiation. To check this possibility, a 27% KNO_3/ZrO_2 sample prepared as a pellet instead of in powder form was used for the XPS test, and as expected the N(1s) signal appeared with considerable intensity as shown in Figure

(18) Daturi, M.; Binet, C.; Bernal, S.; Omil, J. A. P.; Lavalley, J. C. *J. Chem. Soc., Faraday Trans.* **1998**, *94*, 1143.
(19) Folksson, B. *Acta Chem. Scand.* **1973**, *27*, 287.
(20) Tabata, K.; Kamada, M.; Chosom, T.; Nagasawa, Y. *J. Chem. Soc., Faraday Trans.***1998**, 94, 2213.

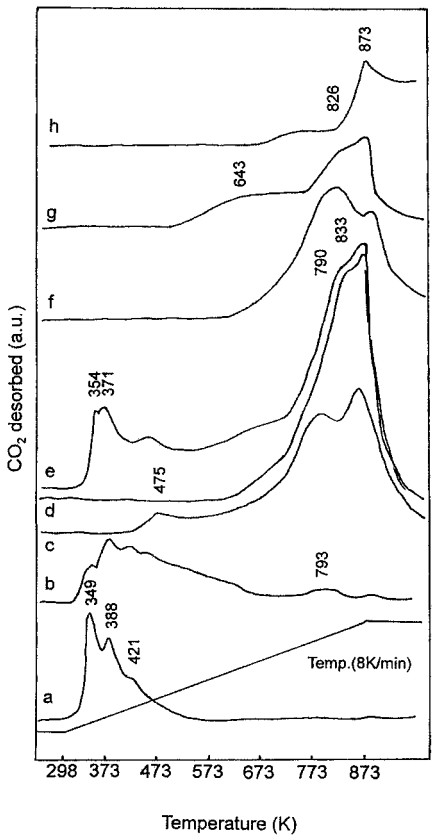

Figure 5. CO_2-TPD spectrum of (a) ZrO_2, (b) 7.5% KNO_3/ZrO_2, (c) 14% KNO_3/ZrO_2, (d) 20% KNO_3/ZrO_2, (e) 20% KNO_3/ZrO_2 but purged with CO_2, (f) 27% KNO_3/ZrO_2, (g) 34% KNO_3/ZrO_2, and (h) KNO_3 unsupported.

4. Radiation of X-ray seems to induce the decomposition of KNO_3 dispersed on a support, even at ambient temperature; therefore, no nitric but only potassium species remained on the surface of composite-loaded KNO_3.

(B) Basicity and Basic Catalytic Properties of KNO_3/ZrO_2 Samples. Figure 5 shows CO_2-TPD spectra of KNO_3/ZrO_2 samples after activation. ZrO_2 had a weak basicity and there were three CO_2-TPD peaks around 349, 388, and 421 K on its spectrum. After supported KNO_3 and activation at 873 K, one new peak of CO_2 desorption emerged on 7.5% KNO_3/ZrO_2 while three appeared around 475, 790, and 873 K on the 14% KNO_3/ZrO_2 sample. The evaluation rate of CO_2 increased on the sample of 20% KNO_3/ZrO_2 above 593 K and gave rise to a peak maximum at 873 K with a shoulder near 833 K. Further addition of KNO_3 on ZrO_2 lowered the maximum temperature of CO_2 desorption from 873 to 823 K, accompanied with a decayed intensity as observed on the 27% KNO_3/ZrO_2 sample. A new peak of CO_2-TPD emerged around 643 K on 34% KNO_3/ZrO_2 while the amount of CO_2 desorbed near 873 K further decreased as seen in Figure 5, owing to the cover of basic sites by the exceeded KNO_3. The introducing manner of CO_2 affected the results of CO_2-TPD. No CO_2 desorbed below 473 K on the samples of ZrO_2-supported KNO_3 more than 14 wt % when the CO_2 was injected in the amount of 400 mL g^{-1}. However, if the sample of 20% KNO_3/ZrO_2 was purged with CO_2 for 2 min prior to the TPD process, desorption of CO_2 below 473 K appeared and indicated the existence of weak basic sites. For comparison KNO_3 was also activated and adsorbed CO_2 under the same conditions. Only one CO_2 desorption near 873 K was observed, resulting from the thermal decomposition of KNO_3 and formation of K_2O species. Consulting these results, most of the strong basic sites on KNO_3/ZrO_2 desorbing CO_2 around 873 K can be attributed to the K_2O extra-fine particles formed on the composites.

Table 3 shows the basicity of the KNO_3/ZrO_2 sample activated at 873 K. The values in the experimental data of the basicity of KNO_3/ZrO_2 were always smaller than the corresponding calculated values, supposing all the KNO_3 converted to K_2O. With these samples in which loaded KNO_3 exceeded 14 wt %, the detected basicity maintained the value 1.35 mmol g^{-1}, very close to the calculated value of 14% KNO_3/ZrO_2 (1.39 mmol g^{-1}). In contrast, the basicity of KNO_3/AlO_3 kept increasing as the amount of KNO_3 rose from 4 to 39 wt %, closely matching the corresponding calculated value. In our opinion, incomplete decomposition of KNO_3 loaded on ZrO_2 results in these differences. Only a part of the loaded KNO_3 could be decomposed during activation, if it had interaction with the carrier or not. If the KNO_3 molecule entered the vacant sites of zirconia, it would be dispersed dissociately and decomposed in the activation process to form basic sites. For those not having interaction with the support, they still kept the original property and needed a high temperature for decomposition. Consequently, the maximum basicity of KNO_3/ZrO_2 is close to the calculated value of 14% KNO_3/ZrO_2 because the KNO_3 that exceeded the spontaneous dispersion threshold cannot contact and have interaction with the support.[4]

Table 3 lists different basicities of KNO_3/ZrO_2 measured by titration and CO_2-TPD methods. With the sample of 7.5% KNO_3/ZrO_2, the value determined by CO_2-TPD (0.06 mmol g^{-1}) was about one-sixth of that by titration (0.35 mmol g^{-1}); for the 14% KNO_3/ZrO_2 sample the corresponding values were 0.14 and 1.14 mmol g^{-1} and the former was about one-eighth of the latter. Another obvious difference could be observed with the 34% KNO_3/ZrO_2 sample where the data measure by CO_2-TPD (0.08 mmol g^{-1}) was only one-sixteenth of that by titration (1.38 mmol g^{-1}). Similar disagreeing results were also found with KNO_3/Al_2O_3 as shown in Table 3 and are attributed to the overlapping structure of basic species formed on the sample.[4] In such an overlapping structure the basic species covered by upper layers was not exposed to CO_2, but would react with an acidic agent if the top layers were resolved in an aqueous titration process. Consequently, the data of CO_2-TPD just designate the amount of basic sites exposed at the top of the overlapped structure while titration data represent the total basicity of the composite; no doubt the former is smaller than the latter.

Figures 6 and 7 show catalytic behaviors of KNO_3/ZrO_2 in the decomposition of propa-2-nol. Catalytic decomposition of propa-2-nol is usually utilized to evaluate the acidic or basic properties of a solid because propa-2-nol can be dehydrated on an acidic site or dehydrogenated over a basic site.[21−24] KNO_3 exhibited

(21) Pines H.; Haag, W. O. *J. Am. Chem. Soc.* **1960**, *82*, 2471.
(22) Noller, H.; Ritter, G. *J. Chem. Soc., Faraday Trans. 1* **1984**, *80*, 275.

Table 3. Basicity of KNO_3/ZrO_2 and KNO_3/Al_2O_3 Samples

sample	amount of KNO_3 loaded (K^+ nm^{-2})	calculated basicity (A) (mmol g^{-1})[a]	measured basicity (mmol g^{-1}) (B)	(C)	B/C	C/A	base strength (H_-)
ZrO_2	0		0.04	0.04	1.00		≤15.0
7.5% KNO_3/ZrO_2	4.0	0.74	0.06	0.35	0.17	0.47	27.0
14% KNO_3/ZrO_2	8.1	1.39	0.14	1.14	0.12	0.82	27.0
20% KNO_3/ZrO_2	12.4	1.98	0.15	1.35	0.11	0.68	27.0
27% KNO_3/ZrO_2	18.4	2.67	0.12	1.38	0.09	0.52	27.0
34% KNO_3/ZrO_2	25.6	3.37	0.08	1.36	0.06	0.40	≤18.4
γ-Al_2O_3	0	0					
4% KNO_3/Al_2O_3	1.4	0.40	0.19	0.39	0.49	0.98	18.4
13% KNO_3/Al_2O_3	4.6	1.29	0.25	1.06	0.24	0.82	27.0
29% KNO_3/Al_2O_3	13.8	2.87	0.27	2.87	0.09	1.00	27.0
39% KNO_3/Al_2O_3	18.5	3.86	0.17	3.62	0.05	0.94	27.0

[a] All of the loaded KNO_3 was assumed to decompose and convert to base such as KOH.

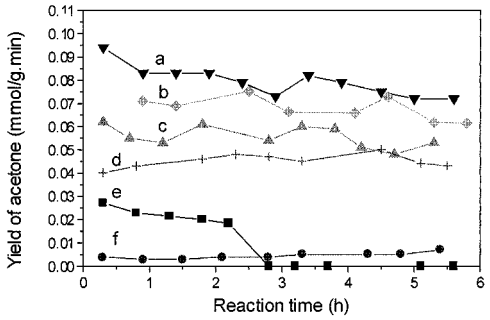

Figure 6. Yield of acetone on the ZrO_2 sample loaded with KNO_3 of (a) 14 wt %, (b) 27 wt %, (c) 7.5 wt %, (d) 34 wt %, (e) 0 wt %, and (f) KNO_3 unsupported in the decomposition of 2-propanol at 673 K.

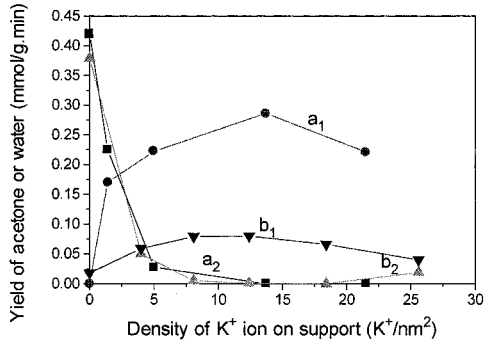

Figure 7. Yield of acetone and water in the decomposition of 2-propanol at 673 K on KNO_3/Al_2O_3 and KNO_3/ZrO_2 via the density of potassium ions loaded. (a) Yield of acetone on KNO_3/Al_2O_3. (b) Yield of acetone on KNO_3/ZrO_2. (c) Yield of water on KNO_3/Al_2O_3. (d) Yield of water on KNO_3/ZrO_2.

both low activity and low acetone selectivity in the reaction at 673 K; only 2% of the reactant converted and the yield of acetone was about 0.005 mmol (g min)$^{-1}$ (Figure 6). Acetone appeared in the reaction products on ZrO_2 within a 2-h run, but disappeared soon as the reaction prolonged. In contrast, the water yield on ZrO_2 was stable and high (0.38 mmol (g min)$^{-1}$) as shown in Figure 7 in that the acid sites of ZrO_2 played a predominant role in propa-2-nol decomposition. After 7.5 wt % KNO_3 was loaded, the acetone yield on ZrO_2 was doubled to about 0.06 mmol (g min)$^{-1}$; meanwhile, the water yield decreased dramatically to 0.05 mmol (g min)$^{-1}$ because acid sites and propa-2-nol dehydration were suppressed. Dispersion of KNO_3 with 14 wt % on ZrO_2 completely suppressed both acid sites and the dehydration of propa-2-nol because no water was detected in the reaction products (Figure 7). In contrast, the acetone yield rose over 0.08 mmol (g min)$^{-1}$ because more basic sites formed on the 14% KNO_3/ZrO_2 sample. Further addition of KNO_3 on ZrO_2 produced no more basic activity for this reaction, and a decayed yield of acetone (curve b in Figure 6) emerged on the sample of 27% KNO_3/ZrO_2. As the loading amount of KNO_3 increased to 34 wt %, water was detected again in the product accompanied with a low yield of acetone (curve d in Figure 6). The re-appearance of dehydrating active sites on the 34% KNO_3/ZrO_2 sample should be attributed to the exceeded KNO_3 because propa-2-nol was preferentially dehydrated over KNO_3 as mentioned above.

KNO_3/ZrO_2 catalysts show stable activity and acetone selectivity in the 6-h run without any tendency toward deactivation. For instance, the propa-2-nol conversion on 14% KNO_3/ZrO_2 was 25.3% at 6 h, similar to that at 1.5 h (26.9%). Besides, the 6-h reaction changed the color of the catalyst from white to slightly gray, which means little coke formed during the run. For the sample 27% KNO_3/ZrO_2 the color became brown after an 8-h run but the activity still remained constant; the conversion at 8 h (21.4%) was close to the value at 1.5 h (22.6%). Unlike those solid acid catalysts on which heavy coke quickly formed to provoke deactivation in the reaction,[25] a solid base like KNO_3/ZrO_2 has a strong ability to repel coking in the catalytic process, which will be important for industry because the cost of regeneration can be thus reduced.

In the isomerization of *cis*-but-2-ene at 273 K probing the strong basicity of the sample,[3] ZrO_2 showed very weak activity while KNO_3 was inactive. Loading KNO_3 onto ZrO_2 dramatically generated high activity for this reaction, as shown in Figure 8, and among them the 14% KNO_3/ZrO_2 sample exhibited the highest activity. No gaseous hydrocarbon other than butenes could be detected in the reaction mixtures and the skeletal isomerization could not be observed. KNO_3/ZrO_2 samples are more active than KNO_3-modified zeolite KL in this reaction. For instance, the initial reaction rate of 7.5% KNO_3/ZrO_2 (3.83 mmol (g min)$^{-1}$) was about 70 times

(23) Hathaway, P. E.; Davis, M. E. *J. Catal.* **1989**, *116*, 263.
(24) Zhu, J. H.; Dong, J. L.; Xu, Q. H. *React. Kinet. Catal. Lett.* **1998**, *63*, 67.
(25) Dong, J. L.; Zhu, J. H.; Xu, Q. H. *Appl. Catal.* **1994**, *112*, 105.

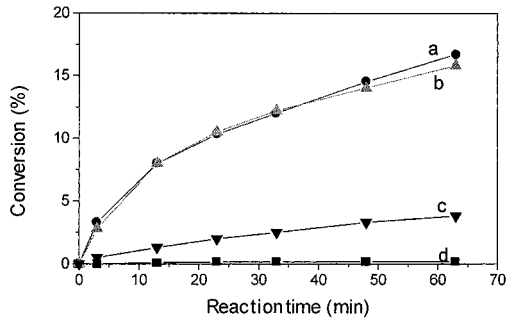

Figure 8. Isomerization of *cis*-but-2-ene on (a) 14% KNO_3/ZrO_2, (b) 20% KNO_3/ZrO_2 (c) 39% KNO_3/ZrO_2, and (d) ZrO_2 at 273 K.

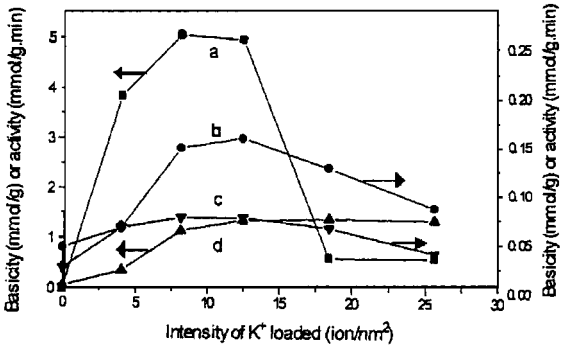

Figure 9. Basicity of KNO_3/ZrO_2 via the amount of KNO_3 loaded. (a) Initial activity in *cis*-but-2-ene isomerization at 273 K. (b) Amount of CO_2 desorbed in the TPD process. (c) Amount of acetone formed in propa-2-nol dehydrogenation at 673 K. (d) Basicity determined by use of titration.

higher than that of 21% KNO_3/KL (0.05 mmol $(g\ min)^{-1}$).[3] This difference results from the composition of the support because the presence of silicon in zeolite hinders the formation of a strong basic site.[26] In addition, Figure 9 demonstrates the relation between basicity and catalytic activity of KNO_3/ZrO_2 samples. The basicity characterized by the amount of acetone formed in propa-2-nol dehydrogenation coincides with that represented by the amount of CO_2 desorbed in CO_2-TPD because only those sites are accessible to reactants and are particularly important for catalysis. Among these basic sites only part of them with strong basicity can catalyze the isomerization of *cis*-but-2-ene at 273 K; for instance, the proportion is about 12% on the sample of 7.5% KNO_3/ZrO_2 estimated from the CO_2-TPD spectrum in Figure 5. Although the catalytic sites were only about 0.007 mmol/g, they were highly active in isomerizing *cis*-but-2-ene, even at 273 K, and provoked an initial rate of 3.8 mmol $(gmin)^{-1}$, which means about nine reactant molecules can be converted on one site per second.

Both double-bond migration and cis−trans isomerization of butene seemed to take place over KNO_3/ZrO_2 samples because the initial ratio of *trans*-but-2-ene to but-1-ene (t-B/1-B) in products was above the unit that is higher than that for the solid base.[27] One may argue if the residual weak acidic sites provoke a high t-B/1-B initial ratio; however, this possibility is excluded considering the dehydration activity of KNO_3/ZrO_2 samples. ZrO_2 exhibited high activity while 20% KNO_3/ZrO_2 was inactive for propa-2-nol dehydration, but a high ratio of t-B/1-B was observed on the latter instead of the former in the isomerization at 273 K. A high t-B/1-B ratio in the products of *cis*-but-2-ene isomerization was also observed on CaO evacuated at 1173 K[28] and KNO_3/Al_2O_3[4] along with KNO_3/KL.[3] This strange phenomenon had been attributed to the existence of superbasic sites because *cis*-but-2-ene could be directly isomerized to *trans*-but-2-ene on these sites at 273 K.[28] On the basis of these facts, two conclusions can be tentatively made. First, the main active sites for isomerization of *cis*-but-2-ene at 273 K are derived from the decomposition products of KNO_3, whether in the form of K_2O ultrafine particles or the K−O−Zr structure in the composite, instead of residual acid sites. Second, superbasic sites exist on the KNO_3/ZrO_2 sample.

Titration with a Hammett indicator confirmed the existence of superbasic sites on KNO_3/ZrO_2 samples. Unlike ZrO_2 showing weak basic properties with a strength of $H_- \leq 15$, the composites derived from KNO_3 and ZrO_2 possess strong basic sites with $H_- = 27.0$ except for 34% KNO_3/ZrO_2 on which only a strength of $H_- \leq 18$ exists (Table 3). According to the definition of Tanabe,[29] these KNO_3/ZrO_2 samples with the basic strength of $H_- = 27.0$ can be regarded as superbases. The structure of a superbasic site is unknown at present. Although a relationship between superbasicity and overlapped structure of basic species has been suggested and supported by some experimental evidence,[4] further study is still desirable to explore the superbasic sites in detail. Discovering superbasicity on KNO_3/ZrO_2 is practically important for industry. These new basic materials are convenient in storage because the interaction between KNO_3 and ZrO_2 is not strong enough to decompose all KNO_3 at ambient temperature. Besides, the activation temperature for KNO_3/ZrO_2 (873 K) is much lower than that for the superbase derived from CaO and SrO (973−1173 K[28]), expanding the way to prepare superbases at low costs.

A comparison of KNO_3/ZrO_2 and KNO_3/Al_2O_3 reveals the complex role of a carrier for supporting KNO_3. (1) Generation of superbasicity on the composite-loaded KNO_3 depends on the vacant sites in the structure of the carrier indeed, and both alumina and zirconia possess a superbasicity with $H_- = 27.0$ after loaded KNO_3. In contrast, no superbasicity was observed on zeolite Y, X, ZSM-5, β, and mordenite, even though they supported KNO_3 and were activated,[3] because of the lack of vacant sites in the framework.[4] (2) The surface state of the carrier strongly influences the final basicity of solid bases derived from supported KNO_3. The hydroxyl group on alumina and zirconia has different acidity[30] owing to the chemical feature of Al^{3+} or Zr^{4+} ions in the oxide carrier, resulting in a different function for the decomposition of KNO_3 along with catalysis in propa-2-nol dehydrogenation (Figure 7). Although the detail mechanism on the effect of the support needs to be explored, selection or synthesis of a suitable carrier

(26) Zhu, J. H.; Chun, Y.; Qin, Y.; Xu, Q. H. *Microporous Mesoporous Mater.* **1998**, *24*, 19.
(27) Foster, N. F.; Cvetanovic, R. J. *J. Am. Chem. Soc.* **1960**, *82*, 4274.
(28) Lizuka, T.; Endo, Y.; Hattori, H.; Tanabe, K. *Chem. Lett.* **1976**, 803.
(29) Tanabe, K.; Noyori, R. *Chokyo-san, Chokyo-enki*; Kodansha: Tokyo, 1980.
(30) Cornet, D.; Burwell, R. L., Jr. *J. Am. Chem. Soc.* **1968**, *90*, 2489.

material is the key step for supporting KNO_3 to prepare a novel superbase.

Conclusions

1. The loading of KNO_3 of 7−27 wt % on ZrO_2 can form superbasic sites with $H_- = 27.0$.

2. A vacant site in the structure of ZrO_2 is crucial for dissociated dispersion and decomposition of KNO_3 to form a basic site so that the spontaneous dispersion capacity of KNO_3 on ZrO_2 is close to the number of vacant sites in ZrO_2. As a result, 14% KNO_3/ZrO_2 appears to have the highest basicity and catalytic activity.

3. KNO_3/ZrO_2 can catalyze a reaction in mild conditions and exhibits high activity for *cis*-but-2-ene isomerization, even at 273 K, because of its unusually strong basicity.

4. KNO_3/ZrO_2 samples show stable activity and selectivity in a catalytic reaction such as decomposition of propa-2-nol at a relatively high temperature because they have the ability to repel coking.

5. With a similar density of potassium ions loaded, KNO_3/ZrO_2 samples possess a smaller basicity and catalytic activity than that of KNO_3/Al_2O_3 because of the smaller vacancies and weaker acidity of the surface hydroxyl group in the former carrier.

Acknowledgment. We are grateful to the Chinese Education Ministry and International Rotary Society (Japan) as well as the Analysis Center of Nanjing University for their financial supports and to Professor T. Yamaguchi in Ehime University (Japan) for his help.

CM000213N